Event-triggered LOS Guidance for Path Following of an Unmanned Surface Vehicle over Wireless Network

Wentao Wu[1], Dan Wang[1], Mingao Lv[1], Jizhou Jiang[1], Lu Liu[1], Zhouhua Peng[1]

1. School of Marine Electrical Engineering, Dalian Maritime University, Dalian 116026, P. R. China

E-mail: {dwang,zhpeng}@dlmu.edu.cn

Abstract: This paper considers kinematic path-following of an under-actuated unmanned surface vehicle (USV) over wireless network. Based on a line-of-sight (LOS) principle, an event-triggered kinematic guidance law is designed to track a predefined path. In order to reduce the communication burden of wireless network, event-triggered mechanisms are introduced to determine the transmission schedules of the vehicle states and the designed commands. The closed-loop kinematic control system is proven to be input-to-state stable. Simulation results demonstrate the efficiency of the event-triggered LOS guidance method for an under-actuated surface vehicle.

Key Words: Path following, under-actuated unmanned surface vehicle, event-triggered mechanism, line-of-sight

1 Introduction

In the past few years, motion control of unmanned surface vehicles (USVs) has received more and more attentions due to their distinctive advantages in numerous military and commercial applications [1–25]. Owing to its little size, light weight, and high speed, USVs are widely used in various mission scenarios such as trajectory tracking [1, 2], target tracking [3–6], path following [7–20], and path tracking [21, 22]. In order to achieve these missions, various guidance methods are proposed including line-of-sight (LOS) [13, 15, 16, 19], constant bearing guidance [23, 24] and pure pursuit guidance [25]. In particular, LOS-based path-following has drawn great attention.

In the literature, path-following of marine vehicles has been widely investigated [7–11, 15–20]. Specially, in [7], the state and output-feedback controllers are developed for coordinated path-following. In [8], a passivity-based synchronization method is presented for synchronized path-following. In [9], the backstepping method and graph theory are used to solve coordinated path-following. In [10], a coordinated path-following method is proposed by using discrete-time periodic communication. In [11], a dynamic surface control (DSC) method based on neural networks are developed for the coordinated path-following under input saturation. In [15], a predictor-based LOS guidance law for path following is proposed estimating the vehicle sideslip angle. In [16], a reduced-order extended state observer (ESO) is employed for LOS guidance law of path following to estimate the sideslip angle. In [17], a output-feedback path-following control method is designed to handle without measuring surge, heave, and pitch velocities. In [18], a performance constrained guidance law formulated with an error transformed function is designed for path-following. In [19], first-order filters and ESOs are employed to design the anti-disturbance path-following controllers. In[20], a neurodynamic optimization technique is employed for path-following to optimize guidance signals in real time. It is worthwhile mentioning that in previous path following controllers, the sample and control are carried out in a periodic manner during communication or actuation which may consume much communication or actuation resources.

Motivated by the above observations, this paper presents an event-triggered kinematic path-following method of an USV in a network environment. In particular, at the kinematic level, an event-triggered guidance law based on the LOS principle is designed to track the known path under the aperiodic communication. The event-triggered mechanisms with the suitable triggering thresholds are developed to reduce the network burden by deciding on the signals transmission between the USV and the remote control center. The stability of the kinematic guidance system is proved by the input-to-state theory. Finally, the simulation results are employed to demonstrate the efficiency of the event-triggered kinematic guidance method.

Compared with the existing works [7–11, 15–19], the obvious contributions of the proposed kinematic guidance method can be concluded as follows. Firstly, this paper proposes the even-triggered kinematic guidance law for an USV over wireless network. One advantage of the guidance method can change the mission of the USV in the remote control center. Secondly, the event-triggered mechanisms are introduced to determine the transmission schedule of the desired signals and the state of the USV. The mechanisms can reduce the communication burden over wireless network.

The contents of this paper are organized as follows. Section 2 introduces the notations. Section 3 gives the problem formulation. Section 4 presents the event-triggered guidance law design and analysis at the kinematic level. Section 5 provides the simulation results for illustrations. Section 6 concludes the paper.

2 Notations

The following notations are frequently used in this paper. $\mathbb{N}$, $\mathbb{R}$ and $\mathbb{R}^+$ present a non-negative integer set, a real set and

This work was supported in part by the National Natural Science Foundation of China under Grants 61673081, 51979020, 51909021, 51939001, and in part by Science and Technology Fund for Distinguished Young Scholars of Dalian under Grant 2018RJ08, and in part by the Stable Supporting Fund of Science and Technology on Underwater Vehicle Technology JCKYS2019604SXJQR-01, and in part by the National Key Research and Development Program of China under Grant 2016YFC0301500, and in part by the Fundamental Research Funds for the Central Universities under Grant 3132019319, and in part by China Postdoctoral Science Foundation 2019M650086.

a positive real set. $(\cdot)^s$ denotes the sample signal. $|\cdot|$ and $\|\cdot\|$ denote the absolute value of a real number and the Euclidean norm of a vector or a matrix, respectively. col$(\cdot)$ and $(\cdot)^T$ are respectively a column vector and the transpose of a matrix. $\lambda_{\max}(\cdot)$ and $\lambda_{\min}(\cdot)$ are the maximum singular value and the minimum singular value of a matrix, respectively.

3 Problem Formulation

According to [15, 26], the kinematics of the USV can be described as

$$\begin{cases} \dot{x} &= \vartheta \cos\psi, \\ \dot{y} &= \vartheta \sin\psi, \\ \dot{\psi} &= \omega + \dot{\beta}, \end{cases} \tag{1}$$

where $x \in \mathbb{R}$ and $y \in \mathbb{R}$ are the positions of the USV in the North-East-Down reference frame $X_E - Y_E$; ψ presents the orientation angle; $\vartheta = \sqrt{u^2 + v^2}$ is the total speed, where u and v denote the surge speed and sway speed in the body-fixed reference frame $X_B - Y_B$, respectively; ω presents the yaw angular velocity; $\dot{\beta}$ is the partial derivative of the sideslip angular $\beta = v/u$.

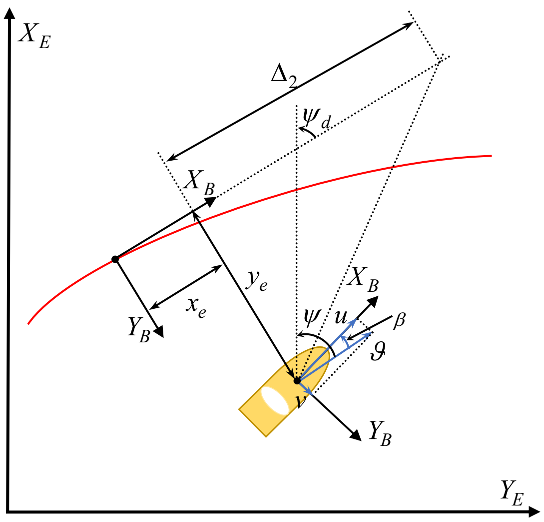

Fig. 1: Line-of-Sight guidance

In the path-following problem, the USV is driven to track the virtual point moving along the predefined parameterized path $p_d(\theta) = \text{col}(x_d(\theta), y_d(\theta))$ with $\theta \in \mathbb{R}$ being a path variable. Then, the tracking errors in the reference frame $X_B - Y_B$ are defined as

$$\begin{cases} x_e &= \cos(\psi_d)(x - x_d) + \sin(\psi_d)(y - y_d), \\ y_e &= -\sin(\psi_d)(x - x_d) + \cos(\psi_d)(y - y_d), \end{cases} \tag{2}$$

where x_e and y_e are respectively the along-track error and cross-track error; $\psi_d = \text{atan2}(\dot{y}_d(\theta), \dot{x}_d(\theta))$ presents the path-tangential angle with $\dot{y}_d$ and $\dot{x}_d$ denoting the partial derivatives of y and x to θ, respectively. The following assumption is needed.

Assumption 1. The parameterized path $p_d(\theta)$ and its first-order partial differentiation $\dot{p}_d(\theta)$ are bounded.

To develop an event-triggered networked path-following guidance law for the USV described with the kinematic model (1), the following control objectives must be satisfied.

i) *Geometric objective*: The along-track error and cross-error can converge to

$$\lim_{t\to\infty} |x_e| \le \delta_1, \text{ and } \lim_{t\to\infty} |y_e| \le \delta_2, \tag{3}$$

where δ_1 and δ_2 are positive constants.

ii) *Velocity assignment*: Define u_0 be the reference velocity of the virtual leader, the objective can be described as follows

$$\lim_{t\to\infty} |\dot{\theta} - u_0| \le \delta_3, \tag{4}$$

where u_0 is a desired update speed of path variable with $u_0 \in \mathbb{R}^+$ and δ_3 is a positive constant.

4 Guidance Law Design and Analysis

In this section, an event-triggered kinematic guidance law is proposed for path-following in a network environment. Next, the event-triggered mechanisms are presented to determine the data transmission over wireless network. Finally, the stability of the kinematic guidance system is analyzed.

4.1 Guidance law design

Using (1), take the time derivative of (2) as follows

$$\begin{cases} \dot{x}_e &= \vartheta \cos(\psi - \psi_d) + y_e \omega_d - \vartheta_d, \\ \dot{y}_e &= \vartheta \sin(\psi - \psi_d) - x_e \omega_d, \end{cases} \tag{5}$$

where $\vartheta_d = u_0\sqrt{x_d'^2(\theta) + y_d'^2(\theta)}$ and $\omega_d = \dot{\psi}_d$.

Define $\varrho_\vartheta = \alpha_\vartheta^s - \alpha_\vartheta$, $\varsigma_\vartheta = \vartheta^s - \alpha_\vartheta^s$, $\varrho_\psi = \alpha_\psi^s - \alpha_\psi$ and $\varsigma_\psi = \psi^s - \alpha_\psi^s$, where α_ϑ and α_ψ are the desired guidance commands. The kinematic tracking error dynamics in (5) can be written as follows

$$\begin{cases} \dot{x}_e &= \alpha_\vartheta^s + \varsigma_\vartheta - 2\vartheta^s \sin^2(\frac{\psi^s - \psi_d}{2}) + y_e^s \omega_d \\ &\quad - \vartheta_d, \\ \dot{y}_e &= \vartheta^s \sin(\alpha_\psi^s + \varsigma_\psi - \psi_d + \beta_s) + \iota - x_e^s \omega_d, \end{cases} \tag{6}$$

where $\iota = \vartheta^s(\sin(\psi^s - \psi_d) - \sin(\alpha_\psi^s + \varsigma_\psi - \psi_d + \beta_s))$.

The following kinematic guidance law is designed to stabilize (2) as follows

$$\begin{cases} \alpha_\vartheta &= -\frac{\mu_1 x_e^s}{\sqrt{(x_e^s)^2 + \Delta_1^2}} + 2\vartheta^s \sin^2(\frac{\psi^s - \psi_d}{2}) \\ &\quad + \vartheta_d, \\ \alpha_\psi &= \psi_d - \beta_s - \arctan(\frac{y_e^s}{\Delta_2}), \end{cases} \tag{7}$$

where $\mu_1 \in \mathbb{R}^+$ is a control gain; $\Delta_1 \in \mathbb{R}^+$ is a constant; $\Delta_2 \in \mathbb{R}^+$ is a look ahead distance.

Let $\varrho_x = x_e^s - x_e$, $\varrho_y = y_e^s - y_e$, $\varrho_\vartheta = \alpha_\vartheta^s - \alpha_\vartheta$ and $\varrho_\psi = \alpha_\psi^s - \alpha_\psi$. By (6) and (7), the dynamics of the errors x_e and y_e can be transformed as

$$\begin{cases} \dot{x}_e = -\mu_1(x_e + \varrho_x)/\Pi_x + \omega_d y_e + \varrho_\vartheta + \varsigma_\vartheta \\ \quad\quad + \omega_d \varrho_y, \\ \dot{y}_e = -\vartheta^s(y_e + \varrho_y)/\Pi_y - \omega_d x_e + \vartheta^s(\varrho_\psi + \varsigma_\psi) \\ \quad\quad + \iota - \omega_d \varrho_x, \end{cases} \tag{8}$$

where $\Pi_x = \sqrt{(x_e^s)^2 + \Delta_1^2}$ and $\Pi_y = \sqrt{(y_e^s)^2 + \Delta_2^2}$.

To achieve coordination, the path update law is designed as follows

$$\dot{\theta} \;\; = u_0 - \mu_2 x_e / \sqrt{x_e^2 + \Delta_3^2}, \tag{9}$$

where μ_2 and Δ_3 are positive constants.

This paper pays close attention to the event-triggered guidance law at the kinematic level. Therefore, we assume that the desired commands can be tracked accurately by the kinetic control law such that $\vartheta = \alpha_\vartheta$ and $\psi = \alpha_\psi$.

4.2 The event-triggered mechanism design

There are two data channels between the remote side and the USV as shown in Fig. 2. Based on the state data required and desired commands released from the remote side, the triggering mechanisms are presented as follows

$$\Omega \begin{cases} \Omega(1): \|\varrho_E\| & = \|E^s(t) - E(t)\| & \leq \varrho_E^*, \\ \Omega(2): \|\varrho_\alpha\| & = \|\alpha^s(t) - \alpha(t)\| & \leq \varrho_\alpha^*, \end{cases} \tag{10}$$

where $E(t) = \mathrm{col}(x_e(t), y_e(t))$, $\alpha(t) = \mathrm{col}(\alpha_\vartheta(t), \alpha_\psi(t))$, $\varrho_E^* \in \mathbb{R}^+$ and $\varrho_\alpha^* \in \mathbb{R}^+$ are predefined triggering thresholds.

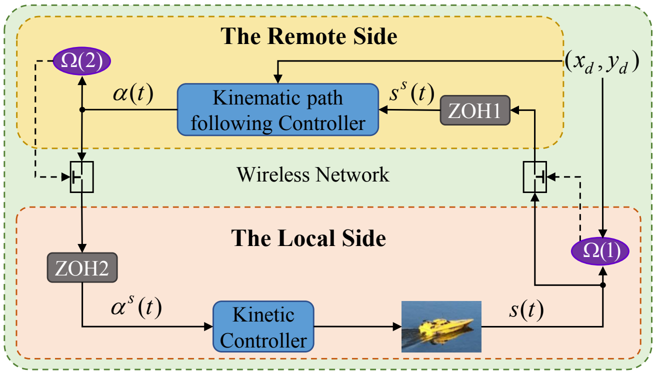

Fig. 2: Kinematic guidance architecture

Define the triggering schedule $t_i^E \in \mathbb{R}^+ (i = \mathbb{N})$ from the USV to the remote side and the triggering schedule $t_j^\alpha \in \mathbb{R}^+ (j = \mathbb{N})$ from the remote side to the USV. Specifically, if the triggering condition $\Omega(1)$ is satisfied at t_i^E, the state of the USV is transmitted to the zero order holder (ZOH) in the remote side over wireless network. During the period $[t_i^E, t_{i+1}^E)$, the kinematic path following controller gives the new desired commands using the sampling state stored in ZHO1. When the condition $\Omega(2)$ is triggered at t_j^α, the current signals are transmitted to the USV for guaranteeing the tracking performance of the USV.

4.3 Stability and Zeno behaviours analysis

The stability of the kinematic guidance system (8) is given by the following lemma.

Lemma 1. The kinematic guidance system (8): $[\varrho_E, \varrho_\vartheta, \varrho_\psi, \varsigma_\alpha, \iota] \mapsto E$ is input-to-stable (ISS).

Proof: Consider a Lyapunov function as $V_1 = (x_e^2 + y_e^2)/2$. Using Take the time derivative of V_1 with (8) as the following

$$\begin{aligned} \dot{V} &= -x_e\mu_1 x_e/\Pi_x - y_e\vartheta^s y_e/\Pi_y - x_e\mu_1\varrho_x/\Pi_x \\ &\quad - y_e\vartheta^s\varrho_y/\Pi_y + \omega_d x_e\varrho_y - \omega_d y_e\varrho_x + y_e\iota + \\ &\quad x_e(\varrho_\vartheta + \varsigma_\vartheta) + y_e\vartheta^s(\varrho_\psi + \varsigma_\psi) \end{aligned} \tag{11}$$

Let $\zeta = \lambda_{\min}(\mu_1/\Pi_x, \vartheta^s/\Pi_y)$, and (11) can be rewritten as follows

$$\begin{aligned} \dot{V} &\leq -\zeta E^T E - E^T(A\varrho_E - \omega_d B_1\varrho_E - B_3\iota - \\ &\quad B_2(\varrho_\alpha + \varsigma_\alpha)) \\ &\leq -\zeta\|E\|^2 + \|E\|(\|A\|\|\varrho_E\| + |\omega_d|\|\varrho_E\| + \\ &\quad \sqrt{1+\vartheta^{s2}}(\|\varrho_\alpha\| + \|\varsigma_\alpha\|) + \|\iota\|) \end{aligned} \tag{12}$$

where $\varrho_E = \mathrm{col}(\varrho_x, \varrho_y)$, $\varrho_\alpha = \mathrm{col}(\varrho_\vartheta, \varrho_\psi)$, $\varsigma_\alpha = \mathrm{col}(\varsigma_\vartheta, \varsigma_\psi)$, $A = \mathrm{diag}(\mu_1/\Pi_x, \vartheta^s/\Pi_y)$, $B_1 = [\begin{smallmatrix} 0 & 1 \\ -1 & 0 \end{smallmatrix}]$, $B_2 = \mathrm{diag}(1, \vartheta^s)$ and $B_3 = \mathrm{col}(0, 1)$. As $\|E\| \geq (\|A\|\|\varrho_E\| + |\omega_d|\|\varrho_E\| + \sqrt{1+\vartheta^{s2}}(\|\varrho_\alpha\| + \|\varsigma_\alpha\|) + \|\iota\|)/(\zeta\kappa)$, it renders that $\dot{V} \leq -\zeta(1-\kappa)\|E\|^2$, where $0 < \kappa < 1$.

By [27], it is concluded that the kinematic guidance system (8) is ISS, and the ultimate bound is given by

$$\begin{aligned} \|E(t)\| &\leq \max\{\|E(t_0)\|e^{-\zeta(1-\kappa)(t-t_0)}, \\ &\quad (\|A\|\|\varrho_E\| + |\omega_d|\|\varrho_E\| + \sqrt{1+(\vartheta^s)^2} \\ &\quad (\|\varrho_\alpha\| + \|\varsigma_\alpha\|) + \|\iota\|)/(\zeta\kappa)\}. \end{aligned} \tag{13}$$

Next, the following theorem explains that Zeno behaviors can be excluded in the remote guidance loop.

Theorem 1. Consider the USV with the kinematics (1) and the event-triggered kinematic guidance law (7). Under the triggering conditions (10), Zeno behaviours can't occur such that $t_E^{i+1} - t_E^i > 0$ and $t_\alpha^{j+1} - t_\alpha^j > 0$.

Proof: Take the time derivative of $\|\varrho_E\|$ over $[t_E^i, t_E^{i+1})$ as $\|\dot{\varrho}_E\| = \|\dot{E}(t)\| \leq -(\zeta + |\omega_d|)\|E\| + (\|A\| + |\omega_d|)\|\varrho_E^*\| + \sqrt{1+\vartheta^{s2}}(\|\varrho_\alpha^*\| + \|\varsigma_\alpha^*\|) + \|\iota^*\|$. By (13), E is bounded. Thence, $\|\dot{\varrho}_E\|$ has an upper bound denoted σ_E. The initial condition satisfies $\lim_{t\to t_E^{i+}} \|\varrho_E\| = 0$. For the time $[t_E^i, t_E^{i+1})$, it has $\|\varrho_E\| \leq \sigma_E(t - t_E^i)$. When the triggering condition $\Omega(1)$ isn't true, the $\lim_{t\to t_E^{(i+1)-}} \|\varrho_E\| = \varrho_E^*$ and it renders $t_E^{i+1} - t_E^i \geq \varrho_E^*/\sigma_E$.

Take the time derivative of $\|\varrho_\alpha\|$ over $[t_\alpha^j, t_\alpha^{j+1})$ as $\|\dot{\varrho}_\alpha\| = \|\dot{\alpha}(t)\| \leq \|\mathrm{col}(\dot{\vartheta}_d, \omega_d)\|$. Because the stability of the remote guidance system is ISS, there is an upper bound of $\|\dot{\varrho}_\alpha\|$ denoted σ_α. The initial condition $\lim_{t\to t_\alpha^{j+}} \|\varrho_\alpha\| = 0$. During $[t_\alpha^j, t_\alpha^{j+1})$, it follows $\|\varrho_\alpha\| \leq \sigma_\alpha(t - t_\alpha^j)$. When $\Omega(2)$ is triggered, the $\lim_{t\to t_\alpha^{(j+1)-}} \|\varrho_\alpha\| = \varrho_\alpha^*$ and it renders $t_\alpha^{j+1} - t_\alpha^j \geq \varrho_\alpha^*/\sigma_\alpha$.The proofs are completed.

5 Simulation Results

In this section, the simulation results are used to illustrate the performance of the proposed event-triggered kinematic path-following method. By [28], the physical parameters of USV is selected and others are presented as follows: $\mu_1 = 1.2$, $\mu_2 = 0.4$, $\Delta_1 = \Delta_3 = 1$, $\Delta_2 = 6$, $\varrho_E^* = \mathrm{col}(0.05\mathrm{m}, 0.05\mathrm{m})$, $\varrho_\alpha^* = \mathrm{col}(0.06\mathrm{m/s}, 0.03\mathrm{rad})$. The predefined path is $p_d = \mathrm{col}(-40+\theta, 40+\theta)$ with $u_0 = 0.2\mathrm{m/s}$, and the initial state of the USV is $s = (x, y, \psi, u, v) = (-85, 0, 0, 0, 0)$.

The simulation results is depicted as Fig. 3 - Fig. 8. The actual tracking performance of the USV is presented by the proposed guidance law in Fig. 3. In Fig. 4, actual and examplng tracking errors are described respectively. Under the event-triggered mechanisms, these errors can still converge to near 0. Fig. 5 and Fig. 6 give the desired and sampling commands. Fig. 7 and Fig. 8 give the kinematic triggering state determined by Ω in the first fifty seconds. According to the triggering state in Fig. 7, we can learn the transmitted schedule of the USV's state. The released schedule of the desired commands can also be known from Fig. 8.

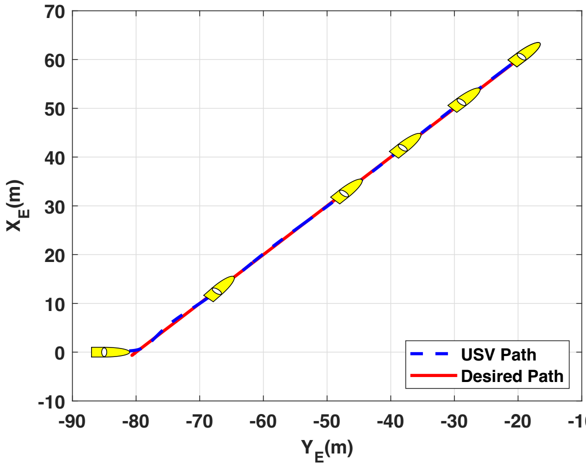

Fig. 3: The performance of the USV

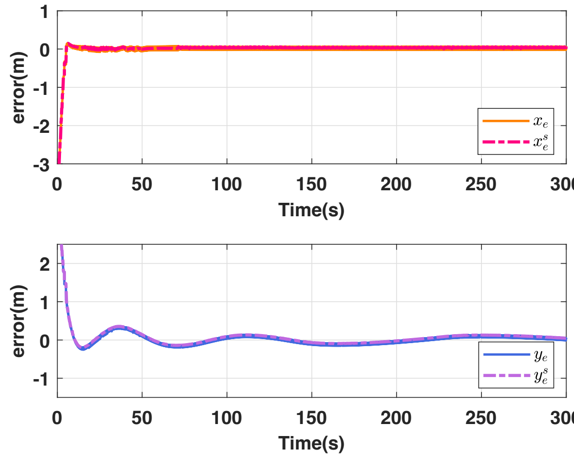

Fig. 4: Along-track and cross-track errors

6 Conclusions

This paper addressed event-triggered path-following of an under-actuated USV at the kinematic level over wireless network. An event-triggered LOS guidance law is designed to achieve path-following. By using predefined triggering mechanisms, the communication burden over wireless network is decreased. The closed-loop kinematic guidance system is proven to be ISS. The simulation results illustrated the effectiveness of the proposed event-triggered LOS guidance method for kinematic path following.

References

[1] Z. Chu, D. Zhu, S. X. Yang, and G. E. Jan, "Adaptive sliding mode control for depth trajectory tracking of remotely operated vehicle with thruster nonlinearity," *Journal of Navigation*, vol. 70, no. 01, pp. 149–164, 2016.

[2] R. Cui, C. Yang, Y. Li, and S. Sharma, "Adaptive neural network control of AUVs with control input nonlinearities using reinforcement learning," *IEEE Transactions on Systems,*

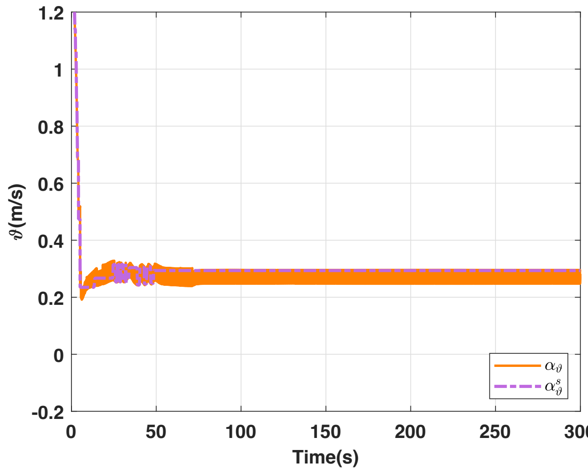

Fig. 5: The desired speed and sampling desired speed

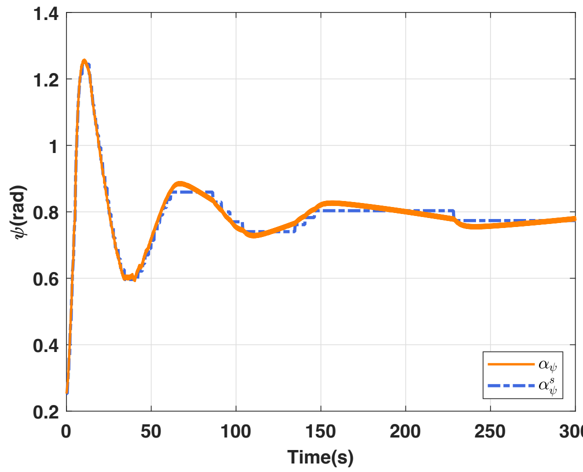

Fig. 6: The desired orientation and sampling orientation

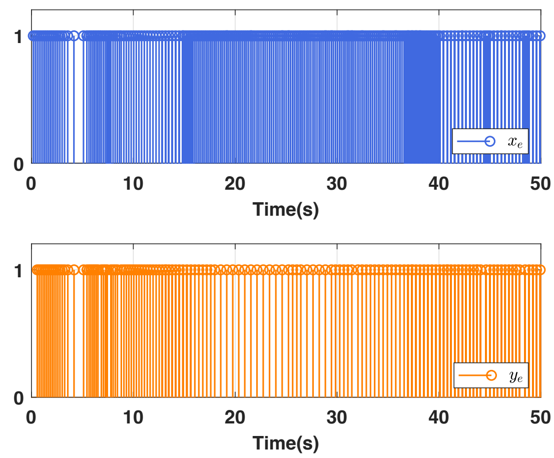

Fig. 7: The triggering state of tracking errors

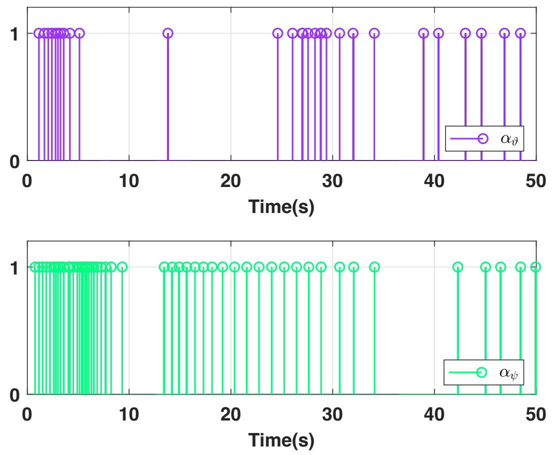

Fig. 8: The triggering state of desired commands

Man, and Cybernetics: Systems, vol. 47, no. 6, pp. 1019–1029, 2017.

[3] R. Cui, S. S. Ge, B. V. E. How, and Y. S. Choo, "Leader-follower formation control of underactuated autonomous underwater vehicles," *Ocean Engineering*, vol. 37, no. 17-18, pp. 1491–1502, Dec 2010.

[4] S.-L. Dai, M. Wang, and C. Wang, "Neural learning control of marine surface vessels with guaranteed transient tracking performance," *IEEE Transactions on Industrial Electronics*, vol. 63, no. 3, pp. 1717–1727, Mar 2016.

[5] L. Liu, D. Wang, Z. Peng, C. L. P. Chen, and T. Li, "Bounded neural network control for target tracking of underactuated autonomous surface vehicles in the presence of uncertain target dynamics," *IEEE Transactions on Neural Networks and Learning Systems*, vol. 30, pp. 1241–1249, 2019.

[6] K. Shojaei and M. Dolatshahi, "Line-of-sight target tracking control of underactuated autonomous underwater vehicles," *Ocean Engineering*, vol. 133, pp. 244–252, 2017.

[7] D. Wang and J. Huang, "Neural network-based adaptive dynamic surface control for a class of uncertain nonlinear systems in strict-feedback form," *IEEE Transactions on Neural Network*, vol. 16, no. 1, pp. 195–202, Jan 2005.

[8] I.-A. F. Ihle, M. Arcak, and T. I. Fossen, "Passivity-based designs for synchronized path-following," *Automatica*, vol. 43, no. 9, pp. 1508–1518, 2007.

[9] J. Almeida, C. Silvestre, and A. Pascoal, "Cooperative control of multiple surface vessels in the presence of ocean currents and parametric model uncertainty," *International Journal of Robust and Nonlinear Control*, vol. 20, no. 14, pp. 1549–1565, 2010.

[10] J. Almeida, C. Silvestre, and A. M. Pascoal, "Cooperative control of multiple surface vessels with discrete-time periodic communications," *International Journal of Robust and Nonlinear Control*, vol. 22, no. 4, pp. 398–419, 2012. [Online]. Available: https://onlinelibrary.wiley.com/doi/abs/10.1002/rnc.1698

[11] H. Wang, D. Wang, and Z. Peng, "Adaptive dynamic surface control for cooperative path following of marine surface vehicles with input saturation," *Nonlinear Dynamics*, vol. 77, no. 1-2, pp. 107–117, 2014.

[12] A. M. Lekkas and T. I. Fossen, "Integral los path following for curved paths based on a monotone cubic hermite spline parametrization," *IEEE Transactions on Control Systems Technology*, vol. 22, no. 6, pp. 2287–2301, Nov 2014.

[13] T. I. Fossen, K. Y. Pettersen, and R. Galeazzi, "Line-of-sight path following for dubins paths with adaptive sideslip compensation of drift forces," *IEEE Transactions on Control Systems Technology*, vol. 23, no. 2, pp. 820–827, Mar 2015.

[14] Y.-Y. Chen and Y.-P. Tian, "Coordinated path following control of multi-unicycle formation motion around closed curves in a time-invariant flow," *Nonlinear Dynamics*, vol. 81, no. 1-2, pp. 1005–1016, Apr 2015.

[15] L. Liu, D. Wang, Z. Peng, and H. Wang, "Predictor-based LOS guidance law for path following of underactuated marine surface vehicles with sideslip compensation," *Ocean Engineering*, vol. 124, pp. 340–348, 2016.

[16] L. Liu, D. Wang, and Z. Peng, "ESO-based line-of-sight guidance law for path following of underactuated marine surface vehicles with exact sideslip compensation," *IEEE Journal of Oceanic Engineering*, vol. 42, no. 2, pp. 477–487, 2017.

[17] Z. Peng and J. Wang, "Output-feedback path-following control of autonomous underwater vehicles based on an extended state observer and projection neural networks," *IEEE Transactions on Systems, Man, and Cybernetics: Systems*, vol. 48, no. 4, pp. 535–544, April 2018.

[18] Z. Zheng and M. Feroskhan, "Path following of a surface vessel with prescribed performance in the presence of input saturation and external disturbances," *IEEE/ASME Transactions on Mechatronics*, vol. 22, no. 6, pp. 2564–2575, 2017.

[19] N. Gu, Z. Peng, D. Wang, Y. Shi, and T. Wang, "Antidisturbance coordinated path following control of robotic autonomous surface vehicles: Theory and experiment," *IEEE/ASME Transactions on Mechatronics*, vol. 24, no. 5, pp. 2386–2396, Oct 2019.

[20] Z. Peng, J. Wang, and Q. Han, "Path-following control of autonomous underwater vehicles subject to velocity and input constraints via neurodynamic optimization," *IEEE Transactions on Industrial Electronics*, vol. 66, no. 11, pp. 8724–8732, 2019.

[21] Q. Zhang, L. Lapierre, and X. Xiang, "Distributed control of coordinated path tracking for networked nonholonomic mobile vehicles," *IEEE Transactions on Industrial Informatics*, vol. 9, no. 1, pp. 472–484, 2013.

[22] K. D. Do, "Synchronization motion tracking control of multiple underactuated ships with collision avoidance," *IEEE Transactions on Industrial Electronics*, vol. 63, no. 5, pp. 2976–2989, May 2016.

[23] M. Breivik and T. I. Fossen, *Guidance Laws for Autonomous Underwater Vehicles*. Rijeka, Croatia: Intech Education, 2009.

[24] Z. Peng, J. Wang, and D. Wang, "Distributed maneuvering of autonomous surface vehicles based on neurodynamic optimization and fuzzy approximation," *IEEE Transactions on Control Systems Technology*, vol. 26, no. 3, pp. 1083–1090, 2018.

[25] W. Naeem, R. Sutton, and s. Ahmad, "Pure pursuit guidance and model predictive control of an autonomous underwater vehicle for cable/pipeline tracking," *IMarEST Journal of Marine Science and Environment, PartC*, vol. 1, 05 2003.

[26] T. I. Fossen and A. M. Lekkas, "Direct and indirect adaptive integral line-of-sight path-following controllers for marine craft exposed to ocean currents," *International Journal of Adaptive Control and Signal Processing*, vol. 31, no. 4, pp. 445–463, 2015.

[27] H. K. Khalil, *Nonlinear Control*. Pearson Education, 2015.

[28] R. Skjetne, T. I. Fossen, and P. V. Kokotović, "Adaptive maneuvering, with experiments, for a model ship in a marine control laboratory," *Automatica*, vol. 41, no. 2, pp. 289–298, 2005.